

DESIGN and FABRICATION of a VIBRATORY MEMS GYROSCOPE BASED ON OUTPUT CURRENT AND BANDWIDTH

Andy Xiao¹, Vaibhav Wanere¹, Vicky Chen¹, Zhongkun Xue¹

¹University of Pennsylvania, USA

ABSTRACT

This paper outlines the design of a vibratory MEMS Gyroscope optimized for minimum output current and bandwidth, achieving 0.1 nA/degree/sec and 50 Hz respectively. A Quality factor (Q) of 100 is attained, with both drive and sense frequencies set at 10 kHz [1] and a drive voltage of 45 V. Utilizing the heightened sensitivity of parallel plate capacitors and the linearity of comb-drive mechanisms, the gyroscope demonstrates enhanced performance. The fabrication process utilizes SiOG (Silicon on glass) for its specific advantages detailed in the paper [2].

INTRODUCTION

This paper introduces a vibratory gyroscope design operating on the principle of Coriolis force [3], featuring two modes: drive and sense. Illustrated in Fig. 2, the structure comprises a drive mass and a sense mass, with the drive mass actuated electrostatically by a comb drive at its resonant frequency. Connected to the substrate via a clamped guided spring structure, the sense mass is linked to the drive mass through a spring, enabling rotation about the z-axis within the established coordinate system. Under sinusoidal voltage excitation, the drive mass oscillates along the x-direction. In the absence of z-axis rotation, both the drive and sense masses oscillate solely in the x-direction. However, when the device rotates at a constant angular speed, the sense mass experiences a Coriolis force determined by the angular rotation rate and its mass. This force induces a displacement in the sense mass, altering the capacitance of parallel plate capacitors formed by the sense mass and stator plates fixed to the substrate. A bias voltage applied across the capacitor facilitates current flow through the circuit, serving as a measure of the angular speed. In this design, the minimum sense current required to measure an angular rate of one degree/sec is 0.1 nA. Additionally, the maximum rotation rate is constrained by the pull-in phenomenon in the parallel plate capacitor, limiting the maximum displacement to $\frac{1}{3}g$, where g represents the gap between the plates.

II. DEVICE DESIGN

The gyroscope design is as shown in Fig. 1 and 2:

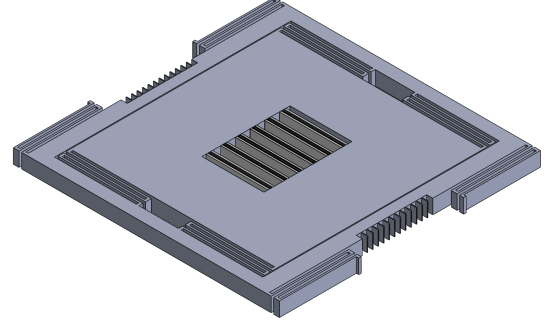


Fig. 1 Isometric View of the Gyroscope Model

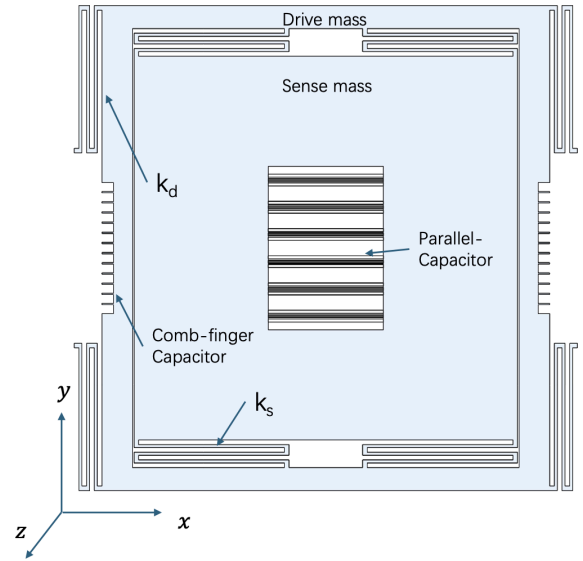


Fig. 2 Top View of the Gyroscope Model

III. CALCULATIONS

The detailed design process is outlined below:

Governing Equation for Sense Side:

$$m\ddot{y} + c\dot{y} + ky = F_{\text{Coriolis}}$$

- A parallel-plate differential transduction was selected for its large transduction coefficients and good sensing for small displacement
- At resonance:

$$c \frac{dy}{dt} = F_{\text{Coriolis}}$$

$$\therefore \frac{dy}{dt} = -2Qx_0\Omega \sin(\omega_0 t)$$

- Sense current is given by:

$$i_c = C(y) \frac{dV_s}{dt} + V_s \frac{dC}{dy} \frac{dy}{dt}$$

- As the bias voltage on the sense side is constant,

$$i_c = V_b (-2Qx_0\Omega \sin(\omega_0 t)) \frac{2C_0}{g}$$

- Current per unit angular rotation rate:

$$\frac{dI}{d\Omega} = V_b (-2Qx_0 \sin(\omega_0 t)) \frac{2C_0}{g}$$

- Since Bandwidth is:

$$BW = \frac{\omega_0}{2Q}$$

- The peak current equation becomes:

$$\frac{dI}{d\Omega_{peak}} = -2V_b x_0 \frac{\epsilon W_c L_c \omega_0}{BW g^2}$$

- The above equation plays a central role in our design given the design goals are to meet minimum current and bandwidth requirements.

- The gap g is limited to min $1.75 \mu\text{m}$ and the width ($35 \mu\text{m}$) is determined by the aspect ratio of 20, both constrained by the fabrication process [2].

- Now, coming to the natural frequency, which is given as:

$$\omega_0 = \sqrt{\frac{k}{m}}$$

- A spring constant range of 70-80 N/m and Natural Frequency of 10 kHz were adopted based on their frequent utilization in MEMS devices [1]. These numbers were then used to calculate the sense mass.

- Subsequently, the dimensions of the sense mass were derived, considering the integration of the sense capacitor within its structure. The maximum length of the capacitor plate, $\max(L_c)$, determines the dimensions of the sense mass.

- Due to the larger drive mass compared to the sense mass, and the requirement of maintaining equal natural frequencies for both components, the spring constant on the drive side must be greater than that on the sense side.

- Peak displacement in the y-direction is given by:

$$y_0 = \frac{2Qx_0}{\omega_0} \Omega$$

- As the bias voltage dictates the pull-in gap, the peak displacement is restricted to $\frac{1}{3}g$. This

limitation imposes an upper bound on the measurable angular speed without experiencing pull-in.

Governing Equation for Drive side:

$$m\ddot{x} + c\dot{x} + kx = F_{\text{drive}}$$

- A comb-finger differential transduction was selected to maximize drive displacement as it is good for driving large displacement at high Q.
- Comb-drive systems were used at both ends of the system to mitigate the effects of bias voltage.
- Peak drive displacement should be at least $2 \mu\text{m}$ and is given by:

$$x_0 = Q \frac{F_{\text{drive}}}{k_{\text{drive}}}$$

- Drive stiffness is determined from drive frequency (same as the sense frequency) and drive mass.

- When $V_B \ll V_{\text{in}}$, the drive force is given by:

$$F_{\text{drive}} = V_B \frac{dC}{dx} V_{\text{in}} = V_B \left(\frac{(N-1)\epsilon h V_{\text{in}}}{g} \right)$$

- Also to achieve the required peak displacement in the x-direction, a large drive force is needed; which was increased by adding more comb fingers.

As a result, the gyroscope's design process was highly iterative and required the application of realistic restrictions resulting from the problem's physics and manufacturing constraints [2]. All the design calculations are available in this [excel workbook](#).

Design Parameters

Parameter	Value
Overall Dimensions (X x Y x Z)	632 μm x 656 μm x 35 μm
Sense Beam Length (x)	190 μm
Number of Sense and Drive Beams in Series	Four parallel springs, each consisting of three beams in series.
Sense/Drive Beam Width	4 μm
Sense Mass	17.7 ng
Sense/Drive Capacitor Gap	1.75 μm

# parallel-plate differential transduction	6 sets
# Sense Stators	12
Sense Stator/Rotor Thickness	35 μm
Sense Stator/Rotor Width	4 μm
Drive Mass	20.4 ng
Drive Spring Length	181 μm
Bias Voltage	40 V
AC Drive Voltage	4 V
Pull In Voltage	48.9 V

Final Design Parameters

Sensitivity @ 1°/sec	2.46 nA
Bandwidth	50 Hz

IV. FABRICATION PROCESS

For the purpose of this device, a SiOG (Silicon on glass) process has been elected to fabricate the gyroscope. While the traditional SOI (Silicon on insulator) process is more established and well-known, thermal expansion mismatch between the silicon structure and packaging material can induce a frequency shift in driving and sensing frequency, therefore degrading the overall performance target we are aiming to achieve. On the other hand, SiOG has been proven to reduce wafer bowing and, subsequently, the mismatch between driving and sensing frequency [2]. As a result, SiOG was chosen to fabricate our gyroscope. The final thickness of a single gyroscope with packaging is 735 μm , while the cross-sectional area is 632 μm x 656 μm . A detailed process flow is described below.

- Starting with a 350 μm thick Pyrex glass wafer, as shown in Fig. 3(a), bottom cavities are fabricated by using a HF wet etch process.
- In Fig. 3(b), 1.75 μm thick aluminum layers are deposited on top of the silicon wafer to serve as an etch stop in the upcoming process.

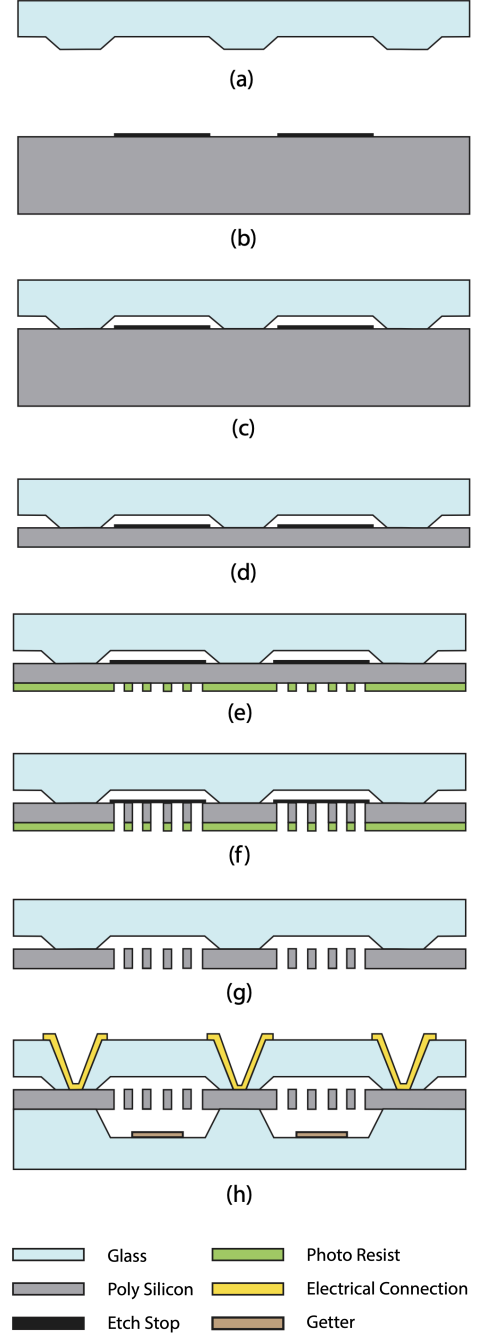


Fig. 3 Fabrication and Packaging of the Gyroscope

- The top glass wafer is combined with the silicon wafer by anodic bonding, as shown in Fig. 3(c).
- Subsequently, the silicon wafer is polished down to our desired thickness of 35 μm by CMP (Chemical Mechanical Polishing), seen in Fig. 3(d).
- In order to fabricate our design feature on the silicon wafer, dark field photoresist is chosen along with the ICP RIE (Inductively coupled plasma reactive ion

etching) process to etch away the silicon, as shown in Fig. 3(e) and (f).

- After the etching process, the aluminum etch stop and photoresist are removed with sulfuric acid and an ashing process, respectively, as shown in Fig. 3(g).
- In Fig. 3(h), another 350 μm thick Pyrex glass wafer was prepared and fabricated cavities with a depth of 160 μm using a similar process.
- Before the bottom glass wafer is combined with the silicon structure, Ti is evaporated to the surface of the glass wafer as a coating in order to reduce and absorb various types of gasses trapped or produced inside the vacuum cavity during the fabrication process, thus ensuring a sufficiently high Q-factor for our purpose.
- Finally, via holes are fabricated using a sandblasting process, after which gold is evaporated onto the via hole surfaces to serve as electrical connections to the silicon structure.

CONCLUSIONS AND FUTURE WORK

A comprehensive design process and fabrication methodology for the vibratory mass gyroscope has been presented. The complexity of the gyroscope design arises from the large number of free variables and concurrent constraints. Furthermore, without a specific application in mind, developing a device that meets application requirements poses a significant challenge. The presented gyroscope demonstrates the capability to measure velocities within the range of 0.166 rpm to 913 rpm. The device has a bandwidth of 50 Hz and 2.46 nA at 1°/sec, with an overall dimension of 632 μm x 656 μm x 735 μm . There exists a discrepancy between the drive and sense frequency caused by the manufacturing constraints that can be mitigated using electrostatic tuning [1]. However, it remains unexplored in this study. This paper serves as a detailed guide to the dimensional design process and lays the groundwork for future research in this area. Additionally, the role of noise in the design process, despite its significance [6], has not been addressed due to constraints on time and knowledge. Further investigation into noise mitigation strategies presents an avenue for future work.

REFERENCES

- [1] F. Pistorio, "Design and FEM Simulation of dual mass resonant MEMS Gyroscope," Masters Thesis, Politecnico Di Torino, 2020.
- [2] Lee, Moon Chul, et al. "A High Yield Rate MEMS Gyroscope with a Packaged SiOG Process." *Journal of Micromechanics and Microengineering*, no. 11, IOP Publishing, Sept. 2005, pp. 2003–10. Crossref, doi:10.1088/0960-1317/15/11/003.
- [3] A. Lawrence, *Modern Inertial Technology*. New York: Springer-Verlag, 1993.
- [4] Aaron Burg, Azeem Meruani, Bob Sandheinrich, and Michael Wickmann, "MEMS Gyroscopes and Their Applications," *Introduction to Microelectromechanical Systems*, pp. 3-20.
- [5] Marc S. Weinberg, "How to Invent (or not Invent) the First Silicon MEMS Gyroscope," *Draper Laboratory*, Cambridge, MA, USA.
- [6] D. Kim and R. M'Closkey, "Noise analysis of closed-Loop vibratory rate gyros," 2012 American Control Conference (ACC), Montreal, QC, Canada, 2012, pp. 92-97, doi: 10.1109/ACC.2012.6314985.